

# 1 On the characteristics of ASCAT wind direction ambiguities

2  
3 **W. Lin<sup>1</sup>, M. Portabella<sup>1</sup>, A. Stoffelen<sup>2</sup>, A. Verhoef<sup>2</sup>**

4 [1]{Institut de Ciències del Mar (ICM) – CSIC, Barcelona, Spain}

5 [2]{Royal Netherlands Meteorological Institute (KNMI), De Bilt, The Netherlands}

6 Correspondence to: W. Lin (wenminglin@cmima.csic.es)

## 7 8 **Abstract**

9 The inversion of the Advanced Scatterometer (ASCAT) backscatter measurement triplets  
10 generally leads to two wind ambiguities with similar wind speed values and opposite wind  
11 directions. However, for up-, down- and cross-wind (with respect to the mid beam azimuth  
12 direction) cases, the inversion often leads to three or four wind solutions. In most of such  
13 cases, the inversion residuals or maximum likelihood estimators (MLEs) of the 3<sup>rd</sup> and 4<sup>th</sup>  
14 solutions (i.e., high-rank solutions) are substantially higher than those of the first two (low  
15 rank) ambiguities. This indicates a low probability for the high-rank solutions and thus  
16 essentially dual ambiguity. This paper investigates the characteristics of ASCAT high-rank  
17 wind solutions under different conditions with the objective of developing a method for  
18 rejecting the spurious high-rank solutions. The implementation of this rejection procedure  
19 improves the effectiveness of the ASCAT wind quality control (QC) and ambiguity removal  
20 procedures.

## 21 22 **1 Introduction**

23 The Advanced Scatterometers (ASCAT) onboard the Metop satellite series are designed to  
24 determine the near-surface winds over the ocean. The first ASCAT onboard Metop-A satellite,  
25 the so-called ASCAT-A, was launched on 19 October 2006. The second onboard Metop-B  
26 satellite, i.e., ASCAT-B, was launched on 17 September 2012. The Ocean and Sea Ice  
27 Satellite Application Facility (OSI SAF) ASCAT-A derived wind products are operational  
28 since February 2007, whereas the OSI SAF ASCAT-B wind products are currently in  
29 development status. ASCAT operates at a microwave frequency of 5.255 GHz (C-band), with

1 three vertically polarized fan beams tracing a swath each side of the sub-satellite track (Figa-  
2 Saldana et al., 2002). In this paper the Wind Vector Cells (WVCs) are numbered from outer  
3 swath to inner swath for both left and right swaths. For instance, WVC number 1 corresponds  
4 to the most outer-swath WVC with highest incidence angle, and WVC number 41 corresponds  
5 to the most inner-swath WVC with lowest incidence angle for 12.5-km ASCAT product. An  
6 important tool for interpreting data is the visualization of the three Normalized Radar Cross  
7 Section (NRCS or  $\sigma^{\circ}$ ) measurements (named triplet) that correspond to the three antenna  
8 beams in 3-dimensional measurement space at each cross-track WVC (Stoffelen and  
9 Anderson, 1997). For a given WVC number, the backscatter signal mainly depends on the  
10 ocean surface wind speed and wind direction, since the parameters of geometrical  
11 measurement are fixed. In the 3D-space visualization, ASCAT measured triplets are  
12 distributed around a well-defined “conical” surface. The latter surface is described by the  
13 forward model or Geophysical Model Function (GMF), which represents the best fit to the  
14 measured triplets.. The GMF relates the backscatter measurements to the observing geometry  
15 and the mean wind vector in a WVC. The radar antenna geometry, the measurement noise, as  
16 well as non-linearities in the GMF complicate the wind retrieval process, which in general  
17 leads to several wind vector ambiguities. The most likely solution is selected with a wind  
18 inversion algorithm. These ambiguities are generally ranked by their probability or distance to  
19 the GMF surface, known as the inversion residual or maximum likelihood estimator (MLE)  
20 (Stoffelen and Portabella, 2006). A spatial filter, the so-called ambiguity removal (AR)  
21 scheme (Stiles et al., 2002; Vogelzang et al., 2009), is then applied to produce the final or  
22 “selected” wind field.

23 Figure 1 shows the distribution of triplets (points) around a cone cross section (double ellipse),  
24 which corresponds to ASCAT WVC number 1, i.e., the inner-most WVC with lowest  
25 incidence angle. Note that the cross section corresponds to a roughly constant wind speed  
26 (e.g., 8 m/s in Fig. 1) whereas the wind direction varies along the double ellipse, such that the  
27 uppermost triplets correspond to winds blowing along the ASCAT mid beam direction  
28 (upwind/downwind or  $0^{\circ}/180^{\circ}$ ), whereas at the lowest points the wind blows roughly across  
29 the mid beam direction (crosswind or  $90^{\circ}/270^{\circ}$ ). The wind inversion minimizes the distance  
30 between the measured triplet and the cone surface. For triplets lying close to the cone surface,  
31 the inversion generally leads to 2 wind solutions or ambiguities  $180^{\circ}$  apart, i.e., two specific  
32 locations on the cone surface minimize the distance due to the double-ellipse shape of the  
33 GMF. Ambiguity removal is generally not difficult in such cases. In contrast, triplets close to

1 the cone centre (and therefore far from the cone surface) generally lead to 3-4 wind solutions.  
2 Such triplets are generally affected by geophysical conditions other than those modelled by  
3 the GMF, such as rain, sea ice, confused sea state and local wind variability, thus leading to  
4 lower quality wind retrievals. A quality control (QC) scheme is used to detect and filter cases  
5 that lead to poor quality retrievals.

6 **Recently we find** that near the up-, down- and cross-wind directions, there are also a  
7 substantial number of triplets which lie close to cone, but have more than two solutions (see  
8 Fig. 1). Besides the first two wind solutions, which correspond to the typical dual ambiguities  
9 derived from triplets near the cone surface, there is a 3<sup>rd</sup> and, in some cases, 4<sup>th</sup> solution  
10 typically in between the 1<sup>st</sup> and 2<sup>nd</sup> solution (at 90°). A 90° shift in wind direction on the cone  
11 surface corresponds to an opposing point, i.e., from up- or downwind to crosswind or vice  
12 versa. According to inversion theory, measured triplets close to the solution surface lead to  
13 good quality wind retrievals. However, the relevance of the additional 3<sup>rd</sup> and 4<sup>th</sup> wind  
14 solutions on the opposing side of the cone has never been assessed. That is, are these so-called  
15 “high-rank” solutions meaningful in terms of probability of being the true wind or rather  
16 artefacts of the inversion procedure?

17 In Section 2, it is shown that some “high-rank” solutions are in fact spurious and should  
18 therefore be removed after inversion (before the ambiguity removal step). In section 3, a  
19 method to distinguish between the “spurious” high-rank solutions and the more credible high-  
20 rank solutions is proposed. Validation of this method is presented in Section 4. Finally,  
21 conclusions and recommendations can be found in Section 5.

## 22 **2 Scatterometer inversion**

23 Currently, the operational C-band GMF is CMOD5n (Hersbach et al., 2007), which is  
24 depicted in a transformed space, namely z-space (Stoffelen and Anderson, 1997), as follow,

$$25 \quad z_s(\theta, \nu, \varphi) = B_0(\theta, \nu)^{0.625} \times [1 + B_1(\theta, \nu)\cos(\varphi) + B_2(\theta, \nu)\cos(2\varphi)] \quad (1)$$

26 where  $\theta$  is the scatterometer incidence angle,  $\nu$  and  $\varphi$  are the ocean surface wind speed and  
27 wind direction w.r.t. radar beam azimuth respectively.  $B_0$  is the dominant term setting the  
28 wind speed scale, while  $B_1$  and  $B_2$  serve to resolve the wind direction. The particular values of  
29  $B_0$ ,  $B_1$  and  $B_2$  are presented in Verhoef et al. (2008). The most common approach used for  
30 scatterometer wind inversion is the maximum likelihood estimator (Cornford et al., 2004;

1 Pierson, 1989; Stoffelen and Anderson, 1997; Stoffelen and Portabella, 2006). For ASCAT,  
2 the following MLE function is minimized (Stoffelen and Anderson, 1997),

$$3 \quad MLE = \frac{1}{3} \sum_{i=1}^3 (z_{mi} - z_{si})^2 \quad (2)$$

4 where  $z_{mi} = (\sigma_{mi}^o)^{0.625}$  is the backscatter measurement of the  $i^{\text{th}}$  beam in z-space, and  
5  $z_{si} = (\sigma_{si}^o)^{0.625}$  is the transformed backscatter simulated through Eq. (1). The inversion can  
6 therefore be interpreted as the search for the minimum distance between the triplet and the  
7 GMF in a transformed 3D measurement space, i.e., the minimum distance between the triplet  
8 and the cone surface (as illustrated in Fig. 1). The retrieved wind solutions are then sorted by  
9 the MLE value, i.e., the first ranked solution corresponds to the lowest MLE value (i.e.,  
10 shortest distance between the triplet and the cone surface), and so on. Note that the lower the  
11 MLE, the higher the probability of being the true wind.

12 The MLE value is a good indicator of the retrieved wind quality (Portabella and Stoffelen,  
13 2001; Portabella et al., 2012a). To improve the ASCAT MLE-based QC, an MLE sign has  
14 been defined by Portabella (2012a) and implemented in the Numerical Weather Prediction  
15 Satellite Application Facility (NWP SAF) ASCAT Wind Data Processor (AWDP). The sign  
16 works as follows: triplets located inside the cone are assigned with a positive MLE value,  
17 while those located outside the cone are assigned with a negative MLE value. Note that since  
18 the cone surface has two manifolds (as represented by the double-ellipse cross section in Fig.  
19 1), the 1<sup>st</sup> and 2<sup>nd</sup> rank ambiguities for a triplet located between the manifolds will have  
20 opposite MLE signs, i.e., the triplet will be considered inside (outside) the cone surface for  
21 the wind solution lying on the outer (inner) cone manifold.

22 As discussed in Sect. 1, when the triplets lie close to the cone surface, the inversion typically  
23 leads to two wind solutions. The solid line in Fig. 2 illustrates the MLE versus wind direction  
24 for one of such cases, where two well-defined minima have similarly low MLE values, i.e.,  
25 equally and highly probable solutions. Such triplets generally lead to high-quality winds after  
26 AR.

27 When triplets lie far away from the cone surface (e.g., triplets located near the centre of the  
28 cross section in Fig. 1), the inversion leads to typically three or four solutions (Portabella and  
29 Stoffelen, 2001) with similar and large MLE values (as illustrated by the dashed line in Fig. 2),  
30 i.e., up to 4 equally-likely wind ambiguities. Moreover, for such cases, the minima are less

1 well defined, as indicated by the low wind direction modulation of the dashed curve in Fig. 2  
2 and thus have low quality. This is an indication of enhanced isotropy of ocean backscatter  
3 conditions, i.e., reduced wind direction skill, which explains the poor quality wind vector  
4 retrieval (Stoffelen and Anderson, 1997).

5 The dotted line in Fig. 2 represents the wind retrieval for a triplet close to the cone surface at  
6 an up-/down-wind location. There are two well-defined minima and two secondary minima.  
7 The former (1<sup>st</sup> and 2<sup>nd</sup> ranked solutions) correspond to high-probability (low MLE value)  
8 wind solutions at up-/down-wind directions and the latter (3<sup>rd</sup> and 4<sup>th</sup> ranked or high-rank  
9 solutions) correspond to low-probability (high MLE value) crosswind solutions. A similar  
10 effect occurs with triplets close the crosswind direction. In this case, the well-defined minima  
11 (1<sup>st</sup> and 2<sup>nd</sup> rank solutions) correspond to crosswind and the secondary minima (high-rank  
12 solutions) to up-/down-wind solutions(not shown in Fig. 2).

13 According to the shape of the MLE cost function curves in Fig. 2, one can clearly discern two  
14 types of distinct behaviour: triplets close to the cone (solid and dotted curves) and triplets far  
15 away from the cone (dashed curve). The former, with well-defined minima, produce high-  
16 quality winds, whereas the latter, with ill-defined minima, represents lower quality winds,  
17 some of which may be rejected. For triplets close to the cone surface at up-/down-wind and  
18 crosswind locations (dotted line), the secondary minima (high-rank solutions) are poorly  
19 defined (broad) and of very low probability compared with the primary (1<sup>st</sup> and 2<sup>nd</sup> rank)  
20 minima (see large MLE difference between primary and secondary minima in dotted curve).  
21 They are actually produced by the particular cone shape at such wind direction locations,  
22 which is driven by the GMF sensitivity to wind changes and the ASCAT observing geometry.  
23 In other words, it seems that such high-rank solutions are spurious (or meaningless) and  
24 should therefore be rejected before the AR step. A method to separate high-rank solutions in  
25 case of enhanced ocean isotropy (i.e., triplets close to the cone centre) from those with  
26 nominal anisotropy (i.e., triplets close to the cone surface at up-/down- and cross-wind  
27 locations) is therefore required.

### 28 **3 Criterion for rejecting high-rank solutions**

29 To discern the characteristics of ASCAT high-rank ambiguities, three and a half years  
30 (September 2008–February 2012) of OSI SAF 12.5-km ASCAT level 2 (L2) wind data are  
31 firstly collocated with the Tropical Rainfall Measuring Mission's (TRMM) Microwave Imager  
32 (TMI) rain data. The collocation criteria for TMI rain data are less than 30-min time and 0.25°

1 spatial distance from the ASCAT measurements. European Centre for Medium-range  
2 Weather Forecasts (ECMWF) winds are also used in the following analysis, which are already  
3 collected in the ASCAT L2 Binary Universal Format Representation (BUFR) data.  
4 Furthermore, a data set with buoy measurements is examined. This data set collocates three  
5 years (March 2009- February 2012) of OSI SAF 12.5-km ASCAT L2 BUFR data with the  
6 wind and precipitation data measured by the tropical moored buoys. The studied buoy data  
7 are provided by the National Oceanic Atmospheric Administration (NOAA) Tropical Ocean  
8 Atmosphere (TAO) buoy arrays in the tropical Pacific, the Prediction and Research Moored  
9 Array in the Atlantic (PIRATA), and the Research Moored Array for African-Asian-  
10 Australian Monsoon Analysis and Prediction (RAMA) located in the tropical Indian Ocean.

11 As initial criterion for the high-rank solution rejection procedure, no rejections are performed  
12 for wind retrievals below 4 m/s. In contrast, above 4 m/s rejections are always performed for  
13 triplets lying outside the cone, i.e., when the MLE of the 1<sup>st</sup> and/or 2<sup>nd</sup> rank are negative (see  
14 Sect. 2). At low wind speed conditions, ASCAT (and scatterometers in general) have poor  
15 wind direction skill (low anisotropy), i.e., low  $\sigma^\circ$  anisotropy or wind direction modulation  
16 (Stoffelen and Anderson, 1997), and thus no dual-ambiguity high-quality wind direction  
17 solutions are expected. On the other hand, for triplets lying outside the cone, which  
18 correspond to good anisotropic backscatter measurements, the retrieved winds are of high  
19 quality, as shown by Portabella (2012a), and should therefore correspond to dual ambiguity  
20 cases.

21 The most challenging part of the algorithm is to discriminate the high-rank solutions in  
22 backscatter conditions with enhanced isotropy from conditions with nominal anisotropy, in  
23 particular for triplets inside the cone. The MLE value can be used for such a purpose. As  
24 discussed earlier in association with Fig. 2, all solutions for triplets near the central axis of the  
25 cone have about the same distance from the GMF surface. As triplets reside closer to the cone  
26 surface, the difference in distance (MLE) between the high-rank solutions and the low-rank  
27 (1<sup>st</sup> and 2<sup>nd</sup> rank) solutions increases. Figure 3(a) shows the ratio between the third-ranked  
28 and the first-ranked MLE (i.e.,  $|MLE_3/MLE_1|$ ) against the vertical position of the triplets with  
29 more than two solutions as shown in Fig. 1. The cross markers indicate that one of the first  
30 two ranked MLE values is negative, while the dot markers present the results for triplets with  
31 positive  $MLE_1$  and  $MLE_2$  (i.e., triplets inside the cone). Note the clear discrimination of  
32 triplets with respect to cone position, which will be further exploited here. A threshold  $T$  is set

1 to reject the meaningless high-rank solutions for those wind retrievals with positive  $MLE_1$  and  
2  $MLE_2$ . Figure 3(b) is the same with Fig.3(a) but for WVC 41.

3 In summary, the high-rank solutions are rejected for wind retrievals with first-ranked wind  
4 speed  $> 4$  m/s for all WVCs, according to the below criterion,

$$5 \quad MLE_1 < 0 \text{ or } MLE_2 < 0 \text{ or } |MLE_3/MLE_1| > T \quad (3)$$

6 Figure 2 shows that most cases with only two solutions reside near the cone surface. High-  
7 rank solutions in case of nominal anisotropy also reside near the cone surface. Therefore, the  
8 rank-1 MLE distributions of these two categories are expected to be similar. The threshold  $T$   
9 is determined by using this constraint. Figure 4 shows the MLE Probability Distribution  
10 Function (PDF) of the first-rank solutions for two-solution cases at WVC number 1, and a  
11 comparison to that of high-rank rejected cases for various thresholds (see legend). The  
12 standard deviation between the PDF of two-solution cases and those cases with rejected high-  
13 rank solutions is presented in the upper-left corner of Fig. 4 as a function of the threshold. The  
14 minimum value, which indicates the best match between the MLE distributions of the two-  
15 solution cases and cases with rejected high-rank solutions, is obtained at  $T=40$  for WVC  
16 number 1. By compromising the differences of the MLE PDFs over diverse WVCs (not  
17 shown), a threshold of  $T=40$  is set for the rejection procedure.

18 Finally, Fig. 5(a) shows the mean vector root-mean-square (VRMS) difference between the  
19 ASCAT retrieved winds and the ECMWF winds, for two-solution cases (solid line), cases  
20 with rejected (dashed line) and kept (cross-marked line) high-rank solutions. Note that only  
21 rain-free cases according to TMI collocations are taken into account. For WVCs located at  
22 outer and middle swath region (WVC number 1-30, high incidence angle), the wind retrievals  
23 with rejected high-rank solutions have similar performance to that of the two-solution cases,  
24 which indicates that the proposed procedure does a good job for rejecting meaningless or  
25 geometry-related high-rank solutions. However, for inner-swath WVCs (WVC number 31-41,  
26 low incidence angle), the mean VRMS of rejected cases increases with WVC number at  
27 higher rate than the two solutions cases, even if the threshold is enhanced to an extremely  
28 high value (not shown). In fact, this increase is mainly due to the poor rejecting performance  
29 at low wind speed (e.g.  $<6$  m/s) conditions, in which the distribution of the ratio  $|MLE_3/MLE_1|$   
30 is much broader for inner-swath WVCs than for outer-swath WVCs. Regarding the wind bias  
31 and standard deviation (SD) (not shown), both the bias and the SD statistics show similar

1 patterns for rejected and accepted high-rank solution cases at the inner swath WVCs,  
2 indicating that the rejection procedure becomes less effective in this swath region.

3 Figure 5(b) presents the same as Fig. 5(a) but using buoy winds instead of ECMWF as  
4 reference. Due to the lack of buoy collocations, all the collocations are examined regardless  
5 whether they are rainy or rain-free samples. Again the mean VRMS of rejected high-rank  
6 cases is comparable with that of two-solution cases, except for the bump around WVC  
7 numbers 29-33, which is due to the very low number of collocations with rejected high-rank  
8 cases.

#### 9 **4 Analysis of the effectiveness of rejecting high-rank solutions**

10 To verify the impact of the high-rank solution rejection procedure on ASCAT wind retrievals,  
11 the number of geometry-related high-rank solutions that would be selected by the 2D-Var AR  
12 module if they were not rejected is examined. This number divided by the total number of  
13 cases with rejected high-rank solutions is denoted by  $R_s$ . Ideally, 2D-Var AR should only  
14 select a geometry-related high-rank solution in very few cases and rather generally “stick” to  
15 either the 1<sup>st</sup> or the 2<sup>nd</sup> rank solution. For example, assuming that the wind direction  
16 uncertainty is characterized by a Gaussian distribution, the proportion of data (wind direction)  
17 values within 45 degrees is 99.73% (or 95.45%) provided that the 2D-Var uncertainty is 15  
18 degrees (or 22.5 degrees). In other words, the percentage of values beyond 45 degrees is  
19 0.26% (or 4.55%). Therefore, if a local wind direction error of 45 degrees may allow the  
20 selection of a high-rank solution, then its probability of occurrence would be approximately  
21 0.3% in case of a 15 degrees 2D-Var uncertainty and 4.5% for 22.5 degrees uncertainty. The  
22 latter uncertainty may occur for low winds, while the former is more typical for winds of  
23 nominal strength. Both TMI rain-free and rainy collocations are studied. Table 1 presents the  
24  $R_s$  results for different WVC number and geophysical conditions. It shows that the ratio  $R_s$   
25 decreases with increasing wind speed as expected. For inner-swath WVCs, the higher  $R_s$  value  
26 indicates that it is not easy to figure out the geometry-related high-rank solutions, probably  
27 due to increased wind direction uncertainty caused by reduced GMF sensitivity for lower  
28 incidence angles.

29 The rejected high-rank solutions are more likely to be chosen by the AR module of L2  
30 processing in rainy areas, as compared to the rain-free cases. Since ECMWF winds do not  
31 resolve wind variability and downdrafts in rainy areas (Portabella et al., 2012b), it is supposed  
32 that the inaccurate background winds may lead to the selection of spurious high-rank

1 solutions through the AR processing. In other words, it is important to reject the meaningless  
2 high-rank solutions, especially for rainy conditions.

3 The validation using buoy data is also examined. Within the total of 86,000 collocations, there  
4 are 6,140 cases with more than two solutions, among which 2,959 are WVCs with rejected  
5 high-ranked solutions according to the procedure in section 3. The  $R_s$  value for the buoy  
6 collocations is 1.1% (i.e., 33 cases with rejected high-rank solutions, but which are selected  
7 by the AR module). Furthermore, within the  $R_s$  determined category, there are 20 cases in  
8 which the first two ranked solutions are closer to the collocated buoy wind than the higher  
9 ranks. For the other 13 cases, the selected high-rank solutions diverge more than 30 degrees  
10 from the buoy wind direction, but are in slightly better agreement with the buoy than the first  
11 two solutions. This is an indication of potential rain-contaminated ASCAT winds. Such poor-  
12 quality cases should be quality-controlled, i.e., all solutions rejected rather than only the high-  
13 rank solutions. Although rejecting high-rank solutions may lead to MLE-based QC passed  
14 WVCs (MLE of first and second-rank solutions is usually low for rejected high-rank cases),  
15 the latter can easily be filtered by the 2D-Var QC, which checks consistency between the  
16 ASCAT wind solutions and the background or 2D-Var analysed field

17 In 16.7% of cases 2D-Var selected a high-rank solution from the cases with kept high-rank  
18 solutions. The mean VRMS difference with the buoy winds is then relatively high and 4.45  
19 m/s, as compared to 2.53 m/s in cases where the first or second-rank solution was selected. In  
20 54.6% of cases the selected high-rank solution was also the closest to the buoy.

## 21 **5 Conclusions**

22 In cases where the ocean return is rather isotropic, inversion of ASCAT backscatter triplets  
23 results in more than two solutions, i.e., high-rank solutions (up to four) emerge due to reduced  
24 wind direction skill (in cases of, e.g., high sub-WVC wind variability, rain contamination,  
25 etc.). These cases are well represented through these additional wind direction ambiguities  
26 and which need to be kept. On the other hand, for ASCAT measurement triplets located close  
27 to the GMF (cone surface), the inversion procedure results in two wind ambiguities, except  
28 for triplets located at up-, down- and cross-wind locations. These additional and artificial  
29 high-rank solutions appear due to the cone geometry, which is driven by the ASCAT  
30 measurement geometry and the GMF sensitivity. To filter out these geometry-related high-  
31 rank solutions an MLE-based method is proposed. The rationale is to reject these meaningless

1 high-rank solutions and avoid the selection of “spurious” ambiguities during the quality  
2 control and ambiguity removal steps.

3 The 3<sup>rd</sup> and 4<sup>th</sup> rank rejection criteria are the following: a) no rejections for ASCAT winds  
4 below 4 m/s (since these are generally cases with poor wind direction skill); and for winds  
5 above 4 m/s, b) reject for triplets outside the cone surface; and c) reject when  
6  $|MLE_3/MLE_1| \geq 40$ , for triplets inside the cone. It is found that the quality (using both  
7 ECMWF and buoy winds as reference) of the less ambiguous (with rejected high-rank  
8 solutions) WVCs is similar to that of the dual-ambiguity cases, whereas the quality of fully  
9 ambiguous (with kept 3<sup>rd</sup> and 4<sup>th</sup> ranks) WVCs is much lower, as expected (since they  
10 correspond to poor quality cases). However, for inner swath WVCs, where the wind direction  
11 skill is somewhat lower, the rejection procedure is less effective, suggesting that no rejections  
12 should be performed for such WVCs below 6 m/s.

13 Rejected high ranks are more likely to be selected by the AR module (denoted as  $R_s$  cases)  
14 over rainy areas than over dry areas, which suggests a more negative effect of such cases in  
15 rainy conditions when not rejected. However, a significant amount of  $R_s$  cases show high-rank  
16 solutions to be (slightly) closer to buoy data than low-rank solutions. This shows a potential  
17 ASCAT rain-contamination effect on ASCAT WVCs. For such cases, a complementary QC is  
18 required since the MLE-based QC does not filter them (triplets are close to the cone surface).  
19 An alternative QC has been recently presented by Portabella (2012b) with promising  
20 preliminary results. However, further work is required to improve ASCAT rain correction and  
21 QC under rainy conditions.

22 In case that more collocations of ASCAT, buoy wind and precipitation data become available,  
23 a quantitative study of the impact high-rank solutions on both AR and QC in L2 processing  
24 will be carried out.

25

## 26 **Acknowledgements**

27 The work has been funded under the EUMETSAT Ocean and Sea Ice (OSI) Satellite  
28 Application Facility (SAF) Associated Scientist project reference CDOP-SG06-VS03. The  
29 software used in this work has been developed through the EUMETSAT Numerical Weather  
30 Prediction SAF.

31

## 1 **References**

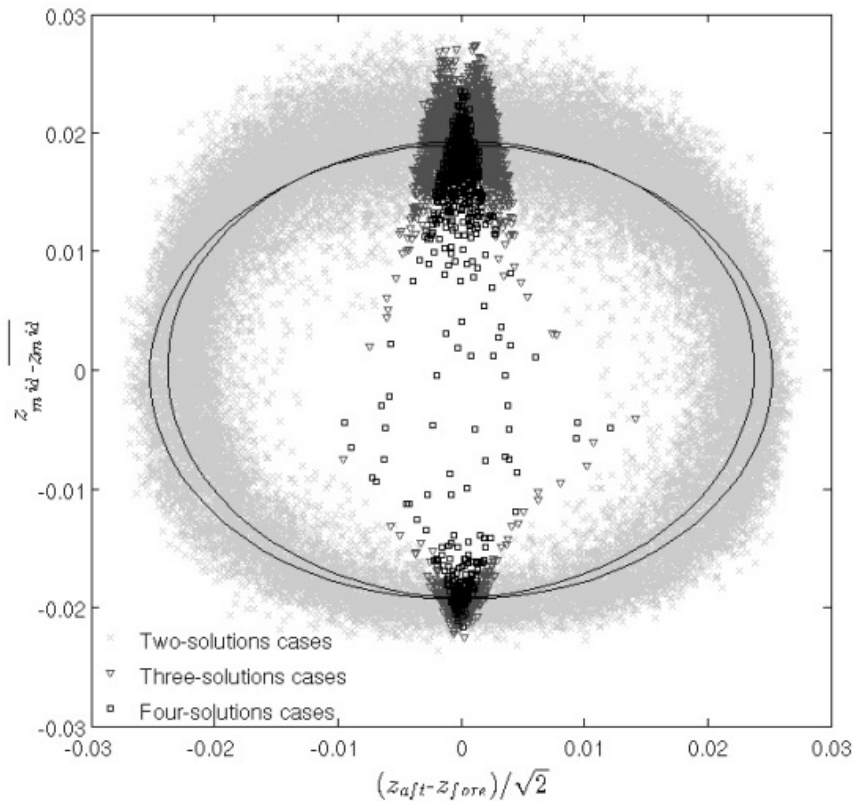
- 2 Cornford, D., Csató, L., Evans, D. J., and Opper, M.: Bayesian analysis of the scatterometer  
3 wind retrieval inverse problems: some new approaches, *J. R. Statist. Soc. B*, 66(3), 609-626,  
4 2004.
- 5 Figa-Saldana, J., Wilson, J. J. W., Attema, E., Gelsthorpe, R., Drinkwater, M.R., and  
6 Stoffelen, A.: The advanced scatterometer (ASCAT) on Metop: A follow-on for European  
7 scatterometers, *Can. Jour. of Rem. Sens.*, 28(3), 404-412, 2002.
- 8 Hersbach, H., Stoffelen, A., and De Haan, S.: The improved C-band ocean geophysical model  
9 function: CMOD-5, *J. Geophys. Res.*, 112, C03006, doi:10.1029/2006JC003743, 2007.
- 10 Pierson, W. J.: Probabilities and statistics for backscatter estimates obtained by a  
11 scatterometer, *J. Geophys. Res.*, 94(C7), 9743-9759, 1989.
- 12 Portabella M. and Stoffelen A.: Rain detection and quality control of SeaWinds, *J. Atmos.*  
13 *Ocean Technol.*, 18(7), 1171–1183, 2001.
- 14 Portabella, M., Stoffelen, Verhoef, A. and Verspeek, J.: A new method for improving  
15 scatterometer wind quality control, *IEEE Trans. Geosci. Remote. Sens. Lett.*, 9(4), 579-583,  
16 2012a.
- 17 Portabella, M., Stoffelen, A., Lin, W., Turiel, A., Verhoef, A., Verspeek, J. and Ballabrera, J.:  
18 Rain effects on ASCAT wind retrieval: Towards an improved quality control, *IEEE Trans.*  
19 *Geosci. Remote Sens.*, 50(7), 2495-2506, 2012b.
- 20 Stiles, B. W., Pollard, B. D., and Dunbar, R. S.: Direction interval retrieval with thresholded  
21 nudging: A method for improving the accuracy of QuikSCAT winds, *IEEE Trans. Geosci.*  
22 *Remote. Sens.*, 40(1), 79-89, 2002
- 23 Stoffelen, A. and Anderson, D.: Scatterometer data interpretation: measurement space and  
24 inversion, *J. Atmos. Ocean. Technol.*, 14(6), 1298–1313, 1997.
- 25 Stoffelen, A. and Portabella, M.: On Bayesian scatterometer wind inversion, *IEEE Trans.*  
26 *Geosci. Remote. Sens.*, 44(6), 1523-1533, 2006.
- 27 Verhoef, A., Portabella, M., Stoffelen, A. and Hersbach, H.: CMOD5.n- the CMOD5 GMF  
28 for neutral winds, *Ocean and Sea Ice SAF Technical Note, SAF/OSI/CDOP/KNMI/TEC/TN/*  
29 *165 v.1, May 2008.*

1 Vogelzang, J., Stoffelen, A., Verhoef, A., De Vries, J. and Bonekamp, H.: Validation of two-  
2 dimensional variational ambiguity removal on SeaWinds scatterometer data, *J. Atmos. Ocean.*  
3 *Technol.*, 26(7), 1229–1245, 2009.  
4

- 1 Table 1. The percentage of triplets with rejected high-rank solutions that selected by the AR
- 2 module. WVC number 1 corresponds to highest incidence angle (outer-most WVC), and
- 3 WVC number 41 corresponds to lowest incidence angle (inner-most WVC)

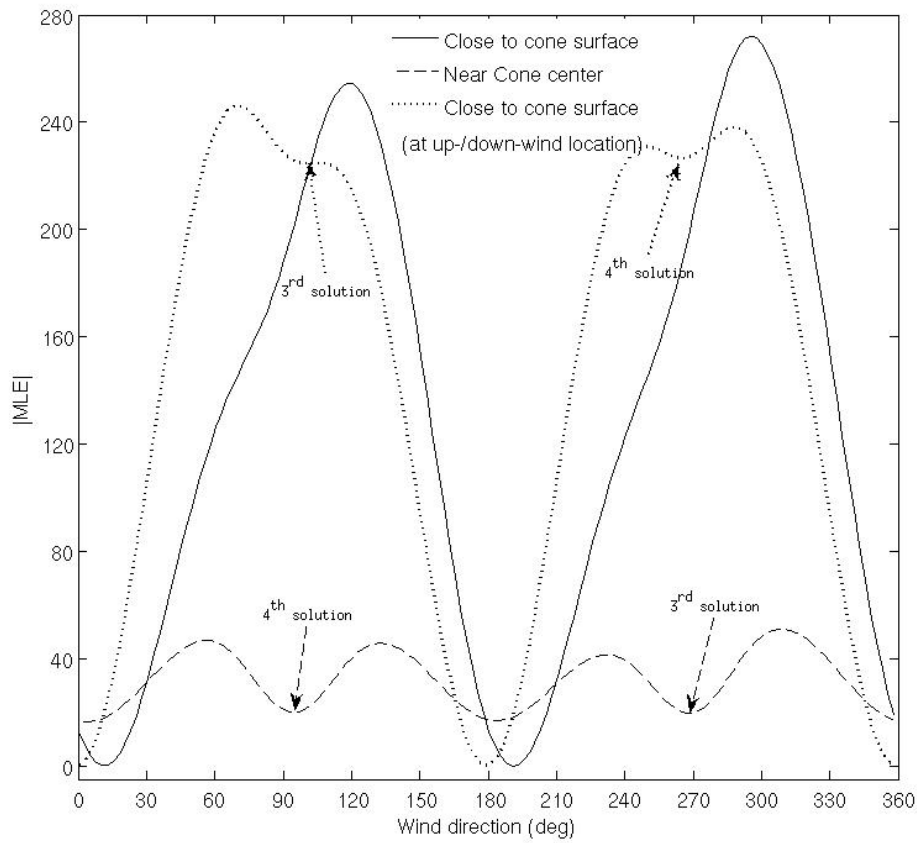
Wind speed (m/s)		$4 < v \leq 6$	$6 < v \leq 10$	$v > 10$
WVC number 1	Rain free	0.3	0.07	0.07
	Rainy	5.3	3.6	3.9
WVC number 41	Rain free	2.2	0.5	0
	Rainy	11.2	6.9	3.2

4



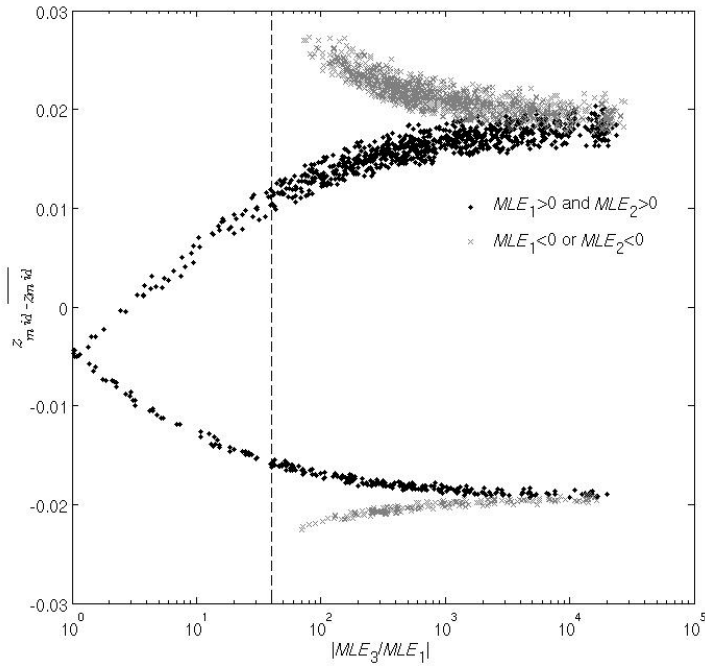
1  
2  
3  
4  
5  
6  
7

Figure 1. Intersection of the cone with plane  $z_{fore} + z_{aft} = 2z_{ref}$  for WVC number 1, for a value of  $z_{ref}$  corresponding approximately to a speed of 8 m/s. Triplets within a distance of  $\pm 0.01 z_{ref}$  from the mentioned plane are plotted. The cross-, triangular- and square-markers in different gray scale represent the triplets with 2, 3 and 4 wind solutions respectively.



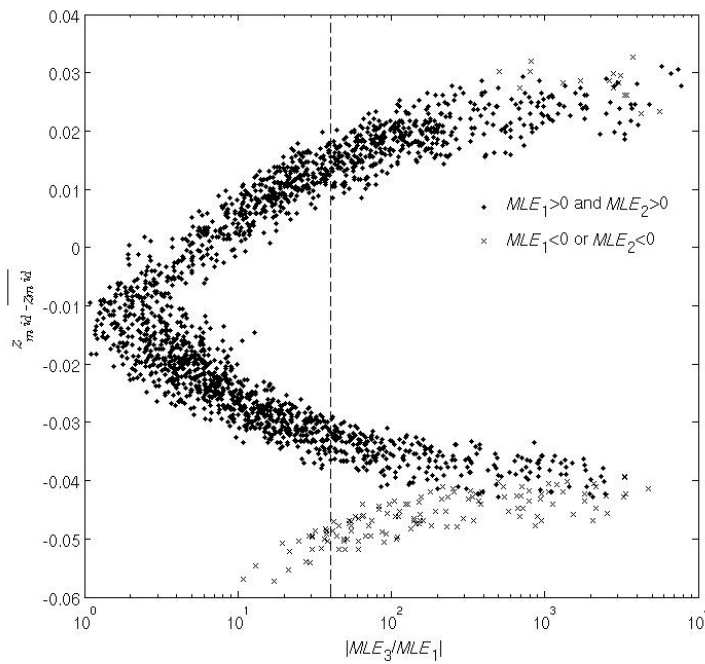
1  
2  
3  
4  
5  
6

Figure 2. Illustration of the  $|MLE|$  versus wind direction during the wind retrieval for three typical cases: triplet close to the cone surface (solid line), triplet near cone centre (dash line), and triplet close to the cone surface at up-/down-wind location.



1

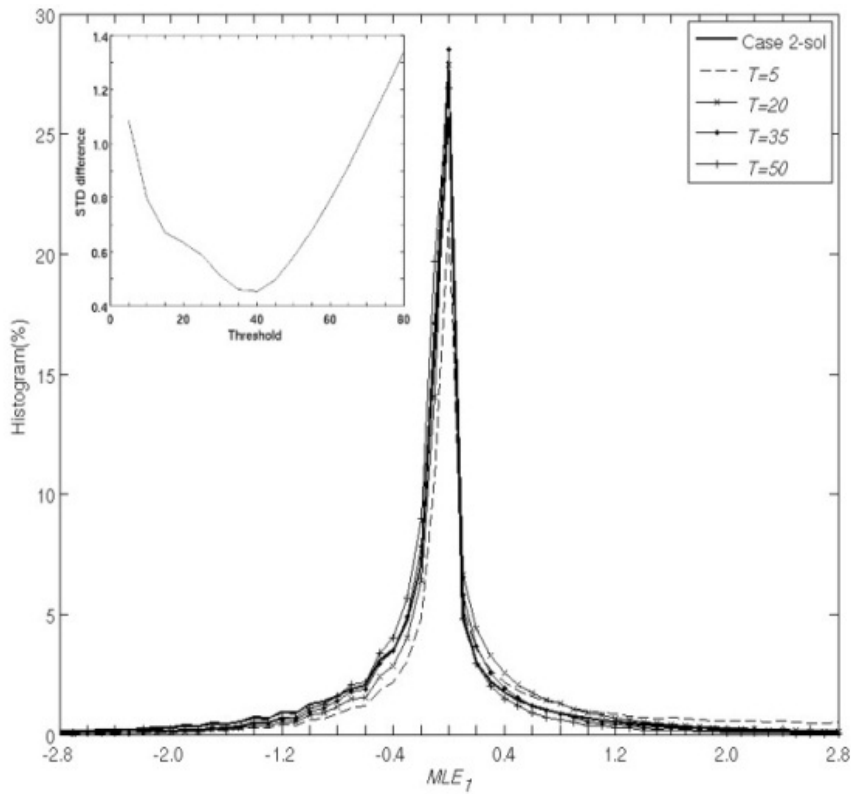
2 (a)



3

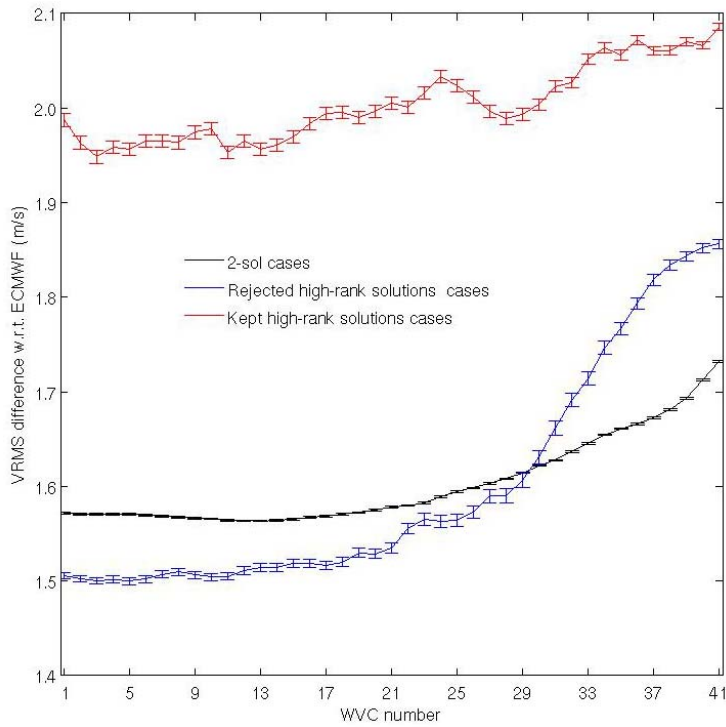
4 (b)

5 Figure 3. (a) Illustration of the ratio  $|MLE_3/MLE_1|$  against the vertical triplet position in Fig. 1  
 6 for triplets with more than two solutions; (b) the same with Fig. 3(a), but for the most inner-  
 7 swath WVC, i.e., number 41. The dashed line indicates the threshold used to separate triplets  
 8 with rejected high-rank solutions (right side) from those with kept high-rank solutions (left  
 9 side).



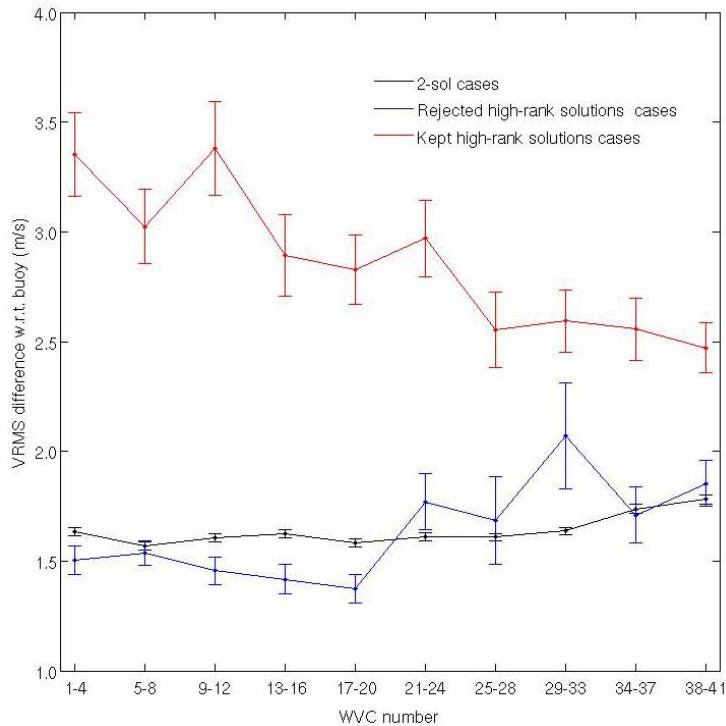
1  
2  
3  
4  
5  
6  
7  
8

Figure 4. Probability Distribution Function of the first ranked MLE at WVC number 1, for two-solution (solid line) and rejected high-rank cases with different thresholds (see legend). The standard deviation between the PDF of the two-solution cases and that of the rejected high-rank cases is illustrated as a function of the threshold in the upper left corner of this figure.



1

2 (a)



3

4 (b)

5 Figure 5. The mean VRMS difference w.r.t. (a) ECMWF winds and (b) buoy winds as a  
 6 function of WVC number, WVCs on both left and right swaths are numbered from 1

- 1 (outermost WVC) to 41 (innermost WVC). Solid line indicates the result of two solutions
- 2 cases, dash line presents the result of cases with rejected high-rank solutions with threshold
- 3  $T=40$ , and cross-marked line illustrates the result of cases with kept high-rank solutions.
- 4 Marker 'I' denotes the uncertainty bar of the estimated mean VRMS for each WVC bin.